Weak-Axis Behavior of Wide Flange Columns Subjected to Blast

Nagarjun Krishnappa[1]; Michel Bruneau, F.ASCE[2]; and Gordon P. Warn, A.M.ASCE[3]

Abstract: Much of past research in the civilian area on the response of civil structures to explosive loading has focused on large detonations in the far field that result in relatively uniform pressure distribution over the structure and specific structural elements. A paucity of research has been conducted that investigates the effect of explosive loading in close proximity to key structural elements. The studies that have been conducted focused primarily on loading perpendicular to the strong axis of bending that result in global deformation, but no rupture or loss of material. Through experimental testing and finite-element simulation, the present study investigates the effect of blast loading on wide flange columns loaded perpendicular to the weak axis of bending. This loading scenario is critical for such columns because the near field shock wave can rupture the web, and in some cases, lead to material loss; both conditions can potentially jeopardize the axial load carrying capacity of the column as a result of increased demands on flanges and possible local buckling of the unrestrained flanges. Therefore, this critical scenario needs to be considered for developing blast resistant measures or assessing the remaining axial and bending capacity of the column. Finite-element simulation can be used for this purpose; the analyses conducted as part of this study replicate, with reasonable accuracy, the experimentally obtained localized deformation, ruptures, and loss of material as a result of blast load, although the finite-element simulation is less successful at replicating the global deformation of the column. **DOI: 10.1061/(ASCE)ST.1943-541X.0000917.**

Author keywords: Wide flange; Column; Blast; Near field; Testing; Simulation; Finite element; Fracture; Analysis and computation.

Introduction

Terrorist attacks and accidental blasts in petrochemical facilities are two scenarios for which it is necessary to consider the protection of civil infrastructure against blast loads. Terrorist threats in North America have often focused on large landmark structures such as suspension bridges (Williamson and Winget 2005). However, government leaders, infrastructure owners, and the engineering community have recognized that the nation's infrastructure system has vulnerabilities and that the collapse of a conventional building or bridge may also result in a significant number of casualties in addition to substantial direct and indirect economic losses. Threat assessment and blast load simulation are two important initial steps in blast resistant design. Many established design documents exist to aid engineers in designing blast resistant structures [ASCE 1997; Department of Defense (DoD) 2008; Dusenberry et al. 2010]; however, the majority of work performed in the development of these documents has focused on far field detonations. A paucity of studies has investigated the response of key structural elements subjected to near field detonations.

Furthermore, past studies investigating the effect of blast loading on wide flange columns have focused on strong axis bending that result in global deformations with no material loss in the section (Karagozian and Case 2005). Although blast loading perpendicular to the strong axis of bending needs to be considered, loading perpendicular to the weak axis is another important scenario for columns because a near field shock wave can rupture the web, leading to material loss resulting in increased axial load demands on the flanges. These increased demands can lead to local buckling of the unrestrained flanges, thus jeopardizing the axial load carrying capacity of the wide flange section. The study by Kazagozian and Case (2005) did include near field detonations on the flange–web intersection region of 0.3-m-long wide flange stubs having continuously supported flanges (laterally restrained); however, these conditions prevent extrapolation of the results to address actual column behavior.

The present study investigates the effect of near field blast loading on wide flange columns loaded perpendicular to the weak axis at different standoff distances through experimental testing and finite-element simulation. Three blast tests were performed on three W14 × 53 propped cantilever columns at varying standoff distances to observe the failure mode and to collect residual deformation data. The residual deformation data were used to investigate the capability of finite-element analysis for replicating the experimental results.

Experimental Testing

Test Specimens

Three blast tests were performed on three different W14 × 53 wide flange propped cantilever columns with near field pressures acting perpendicular to the weak axis of bending. These columns were part of two separate steel plate shear wall (SPSW) frames [Fig. 1(a)]. The tests performed on the wide flange columns were conducted after blast tests were performed on the SPSW infill panels (Warn and Bruneau 2009). The columns [vertical boundary

[1]Structural Engineering, Atkins Global, 920 Memorial City Way, Suite 700, Houston, TX 77024. E-mail: nagarjun.krishnappa@atkinsglobal.com

[2]Professor, Dept. of Civil, Structural and Environmental Engineering (CSEE), Univ. at Buffalo, 130 Ketter Hall, Buffalo, NY 14260. E-mail: bruneau@buffalo.edu

[3]Assistant Professor, Dept. of Civil and Environmental Engineering, Pennsylvania State Univ., 226B Sackett Building, University Park, PA 16802 (corresponding author). E-mail: gpw1@psu.edu

Note. This manuscript was submitted on September 2, 2012; approved on July 23, 2013; published online on July 25, 2013. Discussion period open until May 19, 2014; separate discussions must be submitted for individual papers. This paper is part of the ***Journal of Structural Engineering***, © ASCE, ISSN 0733-9445/04013108(9)/$25.00.

frame (VBE) elements shown in Fig. 1(a)] were visually inspected and measured following the infill tests. The inspection revealed that the wide flange columns showed no signs of residual deformations following the infill tests, indicating that theirs response to the infill tests had been elastic, which was attributed to the relatively large scaled distances between the charge and columns in the infill tests. The infill plates were removed from the frames by using an acetylene torch prior to the blast tests on the wide flange columns.

Only bare columns were tested. This option was selected because: (1) there are many situations in which steel column are exposed, such as parking garages, parking levels in multistory buildings, and atriums; and (2) testing bare columns provides a baseline understanding of the column behavior without the added complexity of cladding/curtain walls, which move the problem from component to system behavior. As such, this research focuses on developing an understanding of component behavior, which is a necessary step toward understanding and modeling the behavior of a system such as a curtain wall–column system. The impact of cladding on the observed column response (local or global deformations) is not speculated here and should be the subject of future research.

The W14 × 53 (SI: W360 × 79) wide flange columns were the VBE elements for two 0.4 length scale SPSW specimens shown in Fig. 1. The length scale factor of 0.4 was dictated by the desire to use a 1.68-m-high existing reaction frame located at the test site. Among the four VBEs, only three were tested in this study. These columns were annotated 1L, 2L, and 2R on the photograph shown in Fig. 1(a) and labeled on the illustration in Fig. 1(b). The infill plates have been removed from the illustration shown in Fig. 1(a) to reflect the fact that they were removed before the column tests. The W14 × 53 columns were cast into a 610 mm wide by 457 mm deep by 4,876 mm long RC foundation beam buried in the ground at the test site [Fig. 1(b)]. The columns were 1.82 m in height and supported by a reaction frame at 1.68 m from the top surface of the foundation. The foundation beam restrained translation and rotation of the base of the column and the reaction frame provided out-of-plane (with respect to the frame) support through bearing so that the boundary conditions for the columns were similar to an

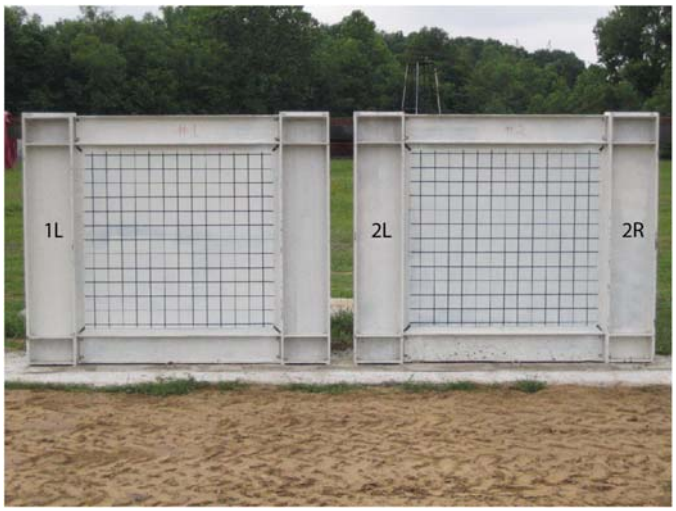

(a)

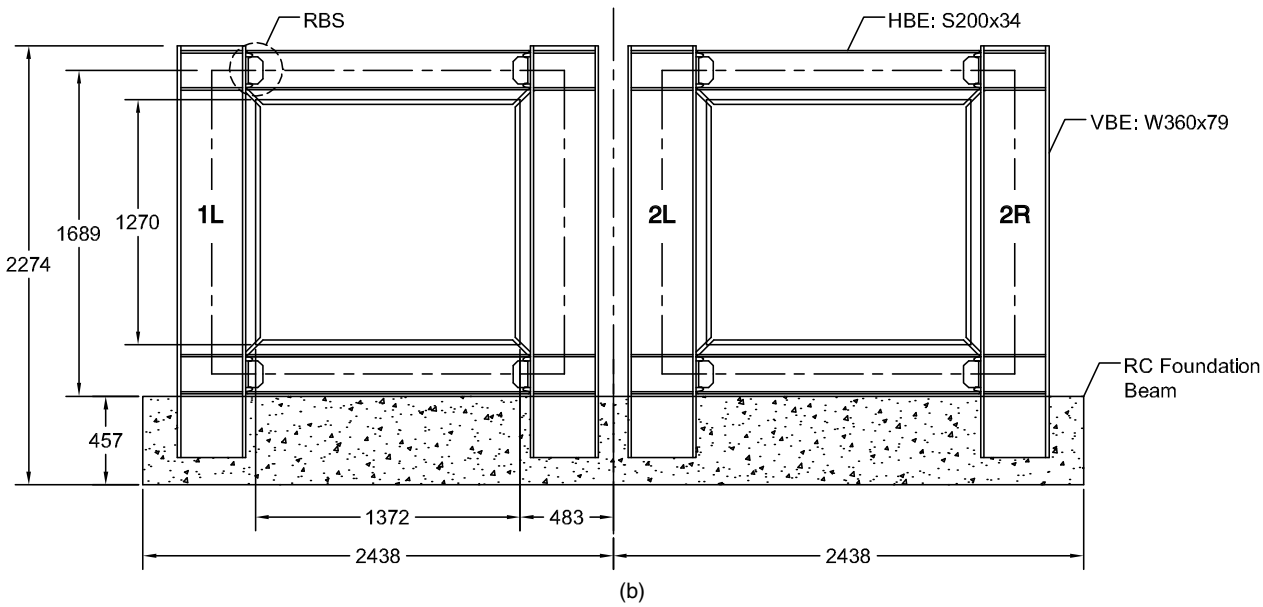

(b)

Fig. 1. Front view of specimens: (a) photograph of SPSW frames and wide-flange columns; (b) illustration of frames with SPSW web plate removed before column tests

idealized propped cantilever. The two columns in each frame were connected directly above the base and at 1.68 m by two S8 × 23 (SI: S200 × 24) horizontal beam elements (HBEs) with an Reduced Beam Section (RBS) connection detail (Warn and Bruneau 2009). The columns were ASTM A992 Grade 50 (ASTM 2011) with a minimum specified yield strength of 348 MPa.

Setup and Test Sequence

Details for each of the three tests are provided in Table 1. The tests were sequenced to prevent loading an adjacent, untested column during any individual test. Specimen 2R (Fig. 1) was tested first (Test 1), followed by Specimen 2L (Test 2) and Specimen 1L (Test 3). For each test, a charge of weight W was located a standoff distance R from the center of the specimen at a height of 0.9 m above the ground surface H, as illustrated in Fig. 2. For each test, the charge weight W remained constant while the standoff distances were varied. Because of security concerns, the charge weight and standoff distances have been omitted from this paper. Although there is no clear-cut definition of a near field detonation, it is generally believed among the engineering community that if the scaled distance Z is less than 0.5 m/kg$^{1/3}$, then the detonation can be considered near field (Pushkaraj 2010), where the scaled distance is determined according to

$$Z = \frac{R}{W^{1/3}} \tag{1}$$

For the three column tests (Table 1), each standoff distance corresponded to a scaled distance less than 0.5 m/kg$^{1/3}$; and each was considered to be a near field detonation.

Observations and Data Collection

A summary of the observations following the tests and the methodology for collecting data are described in this section. Actual, quantitative test results are provided in the section, comparing the experimental data with the results of the finite-element simulation.

Table 1. Summary of Blast Tests on Wide Flange Columns

Test	Specimen	Section size	Charge weight (W)	Standoff distance (R)	Charge height (H) (m)
1	2R	W14 × 53	W	X	0.9
2	2L	W14 × 53	W	1.39X	0.9
3	1L	W14 × 53	W	1.78X	0.9

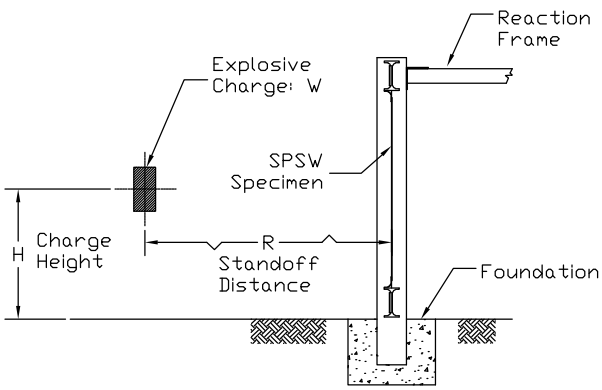

Fig. 2. Illustration of the side view of a specimen showing generic placement of explosive charge

After each test, the columns were visually inspected and residual deformation data were collected. For each test, residual out-of-plane (parallel to strong axis of bending) deformations of the front surface of both flanges and the web along a vertical center centerline covered the entire height of the column. These measurements were taken with respect to a vertical plumb line attached to the 1.7 m height (center of reaction frame) and base of column. In addition, the flange outer face to flange outer face spread was measured along a level line up the entire height of the column, referred to as "face-to-face." The residual deformations were measured at approximately 10-cm increments.

During Test 1, on Specimen 2R, a significant portion of the web material was breached, leaving a large hole in the web of the W14 × 53 column, approximately at midheight of the column, as shown by the photographs in Fig. 3. Significant flange spread was observed, resulting in a hole in the web measuring approximately 0.49 m at the widest point and 0.75 m in height [Table 2; Fig. 3(b)]. Peak out-of-plane deformations of approximately 6 cm were observed at the approximate midheight of the column. The web material could not be found following the test.

Test 2 was performed on Specimen 2L with the same charge weight at a standoff distance 1.39 times that for Test 1. Following Test 2, a large bulge was observed in the web at midheight of the column, as shown in Fig. 4(a). For Specimen 2L, a rupture was initiated near the beam flange intersection, propagating vertically and creating the large bulge visible from the backside of the column, as shown in Fig. 4(a). A rupture on the left side of the bulge is shown in Fig. 4(b). The peak out-of-plane deformation of the flanges on Specimen 2L was approximately 2.5 cm, occurring at the approximate midheight of the column. No significant face-to-face spread of the flanges was observed.

Test 3 was performed on Specimen 1L, using the same charge weight, but at a standoff distance 1.78 times that for

Fig. 3. Photographs of Specimen 2R after Test 1: (a) isometric; (b) front

Table 2. Comparison of Results for Test 1 on Specimen 2R

Results	Height of hole (m)	Relative error (%)	Width of hole (m)	Relative error (%)
Experimental	0.75	0	0.49	0
FE HLSA 350	0.85	13	0.34	30.6
FE C-P	0.83	11	0.34	30.6

Fig. 4. Photographs of Specimen 2L after Test 2: (a) back; (b) front

Test 1. Following Test 3, a bulge deformation, less pronounced than Test 2, was observed in the web at midheight, although no loss of material was observed. Out-of-plane deformation of the column was observed, although it was less noticeable than in previous tests, as shown by the photograph in Fig. 5(a). A peak out-of-plane deformation of the column flanges was measured to be 2.3 cm at midheight. Paint flaking on the backside of Specimen 1L is shown in Fig. 5(b), indicating large plastic strain in the web material at this location.

Finite-Element Simulation

The blast tests on the three wide flange column sections were simulated by using the finite-element (FE) method to assess the ability of such modeling to replicate the experimental results for

Fig. 5. Photographs of Specimen 1L after Test 3: (a) side; (b) back

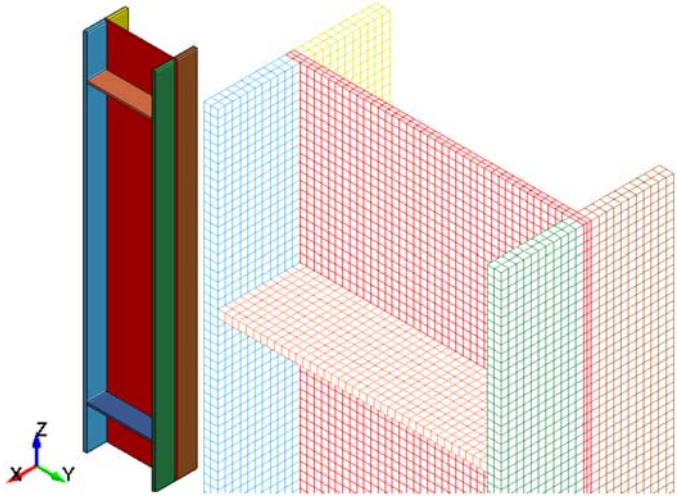

Fig. 6. FE model and mesh of wide flange column

near field detonations. The results of this evaluation will help to determine the adequacy of the FE method and guide future research regarding the level of complexity required to obtain representative results (for example, indicating whether thermomechanical modeling and fluid–structure interaction must be considered).

Near field explosions create rapid and nonuniform overpressures that can lead to strain rates of varying magnitudes across an individual structural element, causing different material response properties over a relatively small dimensional space.

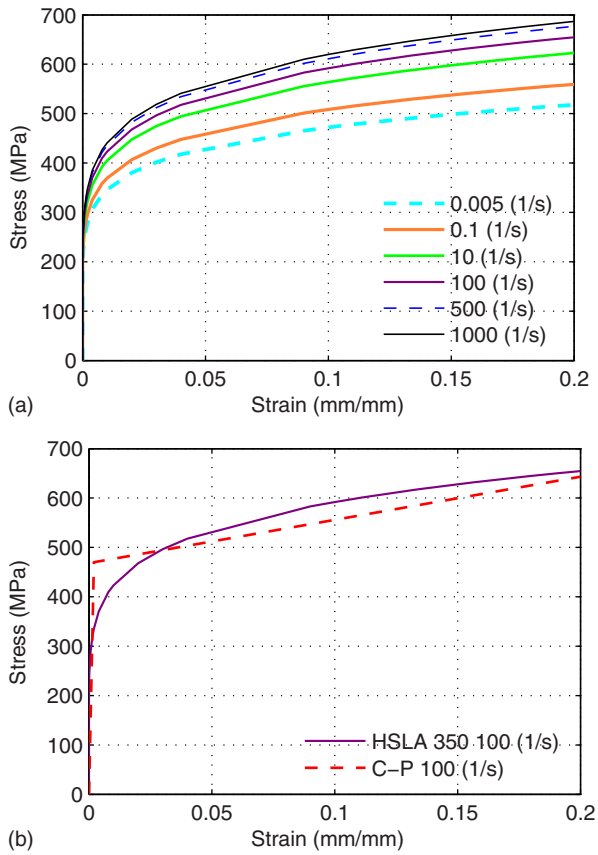

Fig. 7. Stress-strain relationships: (a) HSLA 350 for varying strain rates; (b) comparison of different relationships for a strain rate of 100 (L/s)

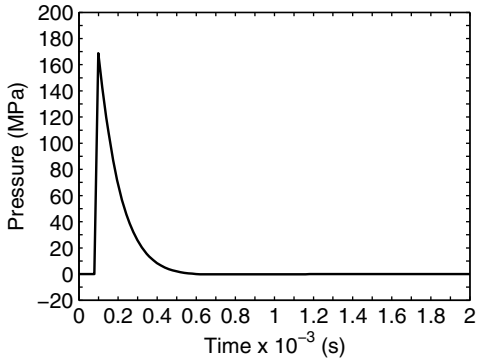

Fig. 8. Reflected overpressure history for the center of the web on the front face at midheight of the column from FE simulation of Test 1

Such explosions can also lead to rupture and material loss, as in the experimental results for Test 1 (Specimen 2R). Material loss and disparate strain rates cannot be accurately simulated by using simplified single degree-of-freedom analyses, which are more appropriate for far field detonations where the overpressures are more uniform in nature. For these conditions, the FE method is required, coupled with computational fluid dynamic (CFD) algorithms. For this study, *LS-DYNA version 971* was chosen to perform all FE analyses.

Model Description

The FE model of the wide flange column was generated by using an assemblage of fully integrated eight-node quadratic brick elements that have both translational and rotational degrees of freedom. The FE model of the W14 × 53 column and mesh are shown in Fig. 6. Two elements were specified through the thickness of the flange and web. The aspect ratio of the flange element was close to unity; however, because of modeling constraints, the aspect ratio of the web elements was 0.5 for the through-thickness dimension.

The boundary conditions of the test column were simulated in the FE model by specifying nodal restraints. All translational and rotational degrees of freedom for the nodes located on the bottom surface of the model were restrained [Fig. 6(a)], effectively simulating a fixed boundary condition. To replicate the lateral restraint provided by the reaction frame (Fig. 2), nodes on the back edge of the column flange at approximately 1.68 m above the base of the column were restrained against translation in the x-direction (Fig. 6). In the test, the column could lift away from the reaction frame because the connection was simply a bearing type connection; however, no separation was observed following the tests, so the nodes at this location were simply restrained in the x-direction.

Material Model

The influence of strain rate on material yield strength and strain hardening can be directly considered in an FE simulation by using material specific stress-strain curves generated for a wide range of strain rates or by using existing models that use empirical relationships developed from testing of similar materials to modify the nominal material properties; i.e., Young's modulus, yield strength, and strain hardening rates. Material testing of the A992 Grade 50 steel (ASTM 2011) specified for the W14 × 53 columns could not be conducted for a sufficiently wide range of strain rates to develop a robust set of stress-strain curves.

Instead, two methods were used to simulate the rate dependency of the steel material. The first method used the Cowper-Symonds (C-P) model available in the *LS-DYNA version 971* library. The C-P model determines the increase in the yield stress as a function of strain rate of loading, according to

$$\frac{\sigma}{\sigma_o} = 1 + \left(\frac{\dot{\varepsilon}}{C}\right)^{1/P} \tag{2}$$

where σ = yield strength determined as a function of the instantaneous strain rate; σ_o = nominal yield strength (measured under

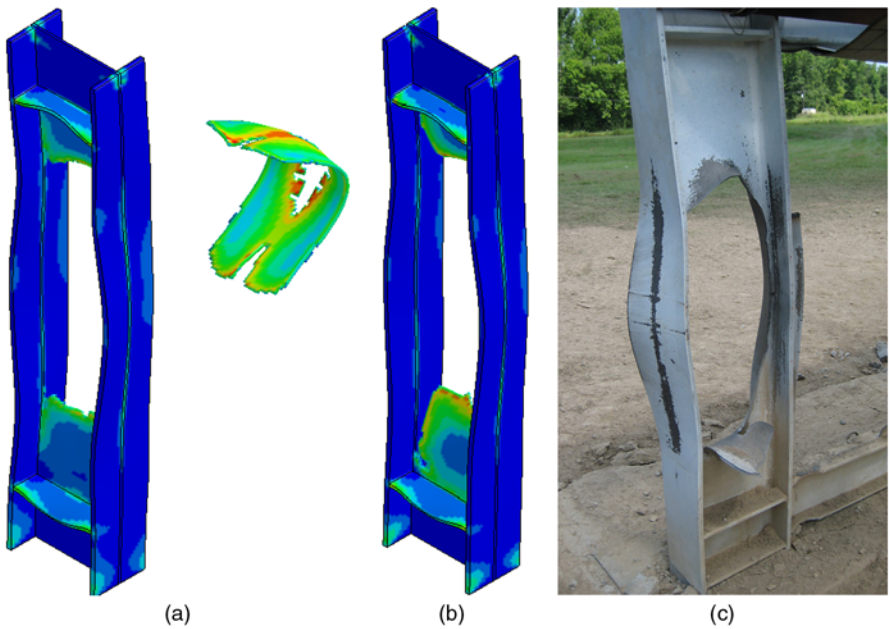

Fig. 9. Qualitative comparison of results: (a) effective plastic strain at 6 m/s using HSLA 350 model; (b) effective plastic strain at 30 m/s using C-P model; (c) observed rupture pattern for 2R following Test 1

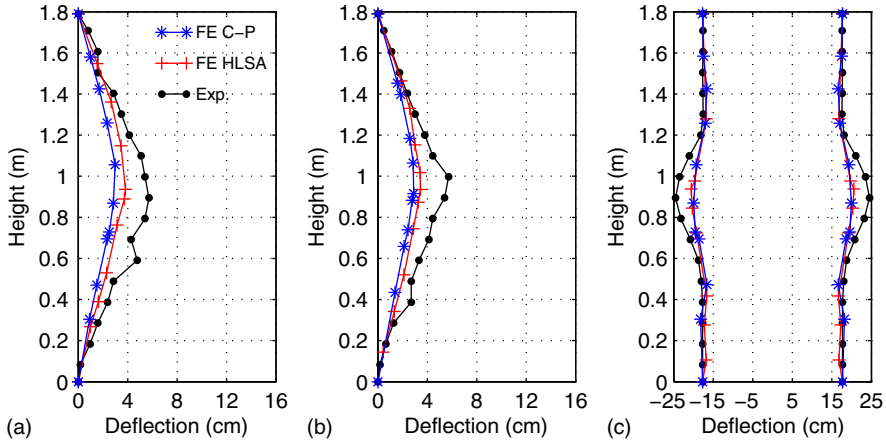

Fig. 10. Comparison of experimental results and FE simulation from Test 1 for Specimen 2R: (a) left flange deflection; (b) right flange deflection; (c) flange spread

quasi-static loading conditions); $\dot{\varepsilon}$ = instantaneous strain rate; C = model parameters; and P = model parameter. A value of 4.41 was specified for P based on tests performed by a World Trade Center (WTC) task committee (Luecke et al. 2005) that recommended this value for all grades of steel, including ASTM A992 Grade 50 (ASTM 2011). The same WTC task committee (Luecke et al. 2005) recommended the following relationship, developed based on the results of tests performed with various samples of steel

$$\log_e C = C_o + C_1\sigma_o + C_2\sigma_o^2 \tag{3}$$

where C_o, C_1, and C_2 = empirical parameters with recommended values of −4.7374, 0.0614, and −0.00171, respectively (Luecke et al. 2005). Using the recommended values for constants C_o, C_1, and C_2 and a nominal yield strength of 348 MPa for ASTM A992 Grade 50 (ASTM 2011), C was found to be 8,648 by using Eq. (3).

The second method is based on an experimental data set for a high strength low alloy (HSLA) steel (Yan and Urban 2003), referred to herein as HLSA 350. Impact testing was performed with coupons made of steel with a similar composition to ASTM A992 grade (ASTM 2011), for the Department of Energy by the American Iron and Steel Institute (Yan and Urban 2003). The HSLA steel was found to have a yield strength of approximately 350 MPa, similar in magnitude to the minimum specified yield strength for ASTM A992 Grade 50 (ASTM 2011); therefore, the HSLA 350 experimental data set was judged to be appropriate for simulating the blast testing performed on the wide flange columns. Stress-strain curves generated from the HSLA 350 data set for strain rates ranging from 0.005 to 1,000 L/s to a maximum strain of 0.2 are presented in Fig. 7(a). For comparison, the stress-strain relationship generated from the C-P model and the HLSA 350 data for a strain rate of 100 L/s are presented in Fig. 7(b).

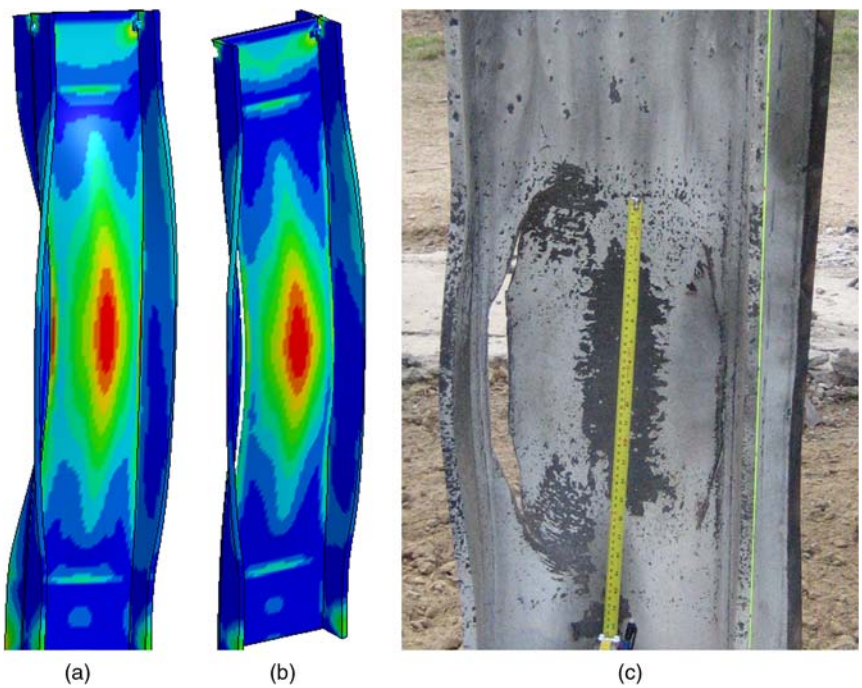

Fig. 11. Qualitative comparison of results: (a) effective plastic strain at 12 m/s using HSLA 350 model; (b) effective plastic strain at 12 m/s using C-P model; (c) observed rupture pattern for 2L following Test 2

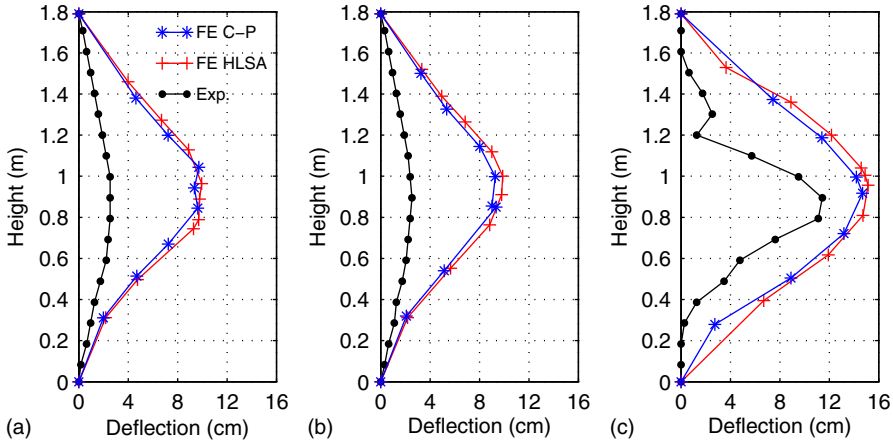

Fig. 12. Comparison of experimental results and FE simulation from Test 2 for Specimen 2L: (a) left flange deflection; (b) right flange deflection; (c) flange spread

Simulated Blast Loading

Time varying pressures were applied to the FE model in *LS-DYNA version 971* by using the Conventional weapons, i.e. CONWEP, air blast function module. To simulate the blast loading, the "load_blast_enchanced type 2" function was selected in *LS-DYNA version 971*, which corresponds to a conventional spherical air blast. The scaled distances for each test were within the recommended range for the "load_blast_enhanced type 2" function. The Friedlander equation was chosen to describe the blast pressure history. However, the charge used in the experiments was cylindrical, with an aspect ratio (diameter/length) of 0.5. As a result, for a charge of the same weight in TNT equivalent, the peak pressures generated by *LS-DYNA version 971* underestimated those calculated by using the *Bridge Explosive Loading (BEL) version 1.1.0.3* developed by the U.S. Army Corps of Engineers, which is able to consider different charge shapes, including cylindrical shapes. To account for the different shape of the charge, the charge weight in *LS-DYNA version 971* was increased so that the peak pressure in *LS-DYNA version 971* matched the peak pressure obtained from *BEL version 1.1.0.3*. However, the duration of the impulse could not be modified because CONWEP uses standard empirical equations that determine the parameters of the blast wave for a given scaled distance and specified weight. The pressure at a point within a Eulerian domain (the air surrounding the section) can be tracked by using a tracer in *LS-DYNA version 971*. For the FE simulations conducted in this study, the air surrounding the column was modeled by using a Eulerian mesh. The pressures from the CONWEP module were applied onto the outermost layer of air (ambient layer) and the pressures were transferred through an inner air layer to the solid elements. The advantage of the ambient air layer approach is the substantial reduction in computational resources and time because the entire air domain between the charge and solid model need not be explicitly considered. The ambient air layer was used to attempt to capture the interaction between fluids and structure occurring in the void between the flanges. A nonreflecting boundary was specified because the surface beneath the charge was soil and the surface in front of the specimens was freshly disturbed soil. To illustrate the intensity of the explosive charge used in this study, the reflected overpressure history for the center of the web at the midheight of the column from the FE simulation of Test 1 is presented in Fig. 8. The reflected overpressure history shown in Fig. 8 has a peak value of 168 MPa at 0.0001 s, after which the pressure decays exponentially with a negative phase, although the magnitude of the negative pressure is quite small, so the negative phase is not readily apparent in the plot.

Comparison of Results

Results from the FE simulation using the C-P material model and the HSLA 350 data generated for each of the three tests are compared with the experimental residual deformation data to evaluate the capability of the FE approach used in this study for replicating the response of wide flange columns subjected to a near field detonation of high explosives.

Test 1: Specimen 2R

The rupture (hole) in the web of Specimen 2R that was observed following Test 1 was also observed in the FE simulation using both the HSLA 350 data and the C-P model. Renderings from the FE analysis using the HLSA 350 data and C-P model are shown in Fig. 9 with a photograph of Specimen 2R following Test 1 [Fig. 9(c)]. The renderings for the HLSA 350 and C-P models were taken

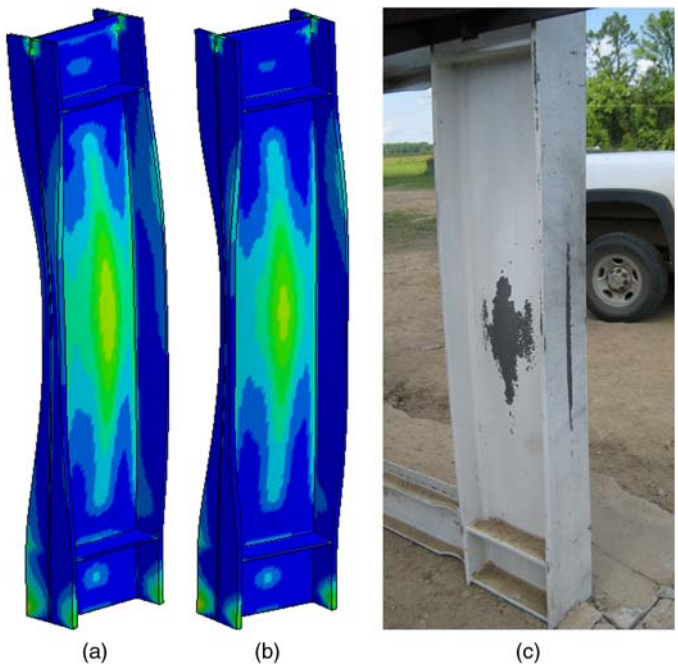

Fig. 13. Qualitative comparison of results: (a) effective plastic strain at 12 m/s using HSLA 350 model; (b) effective plastic strain at 12 m/s using C-P model; (c) observed rupture pattern for 1L following Test 3

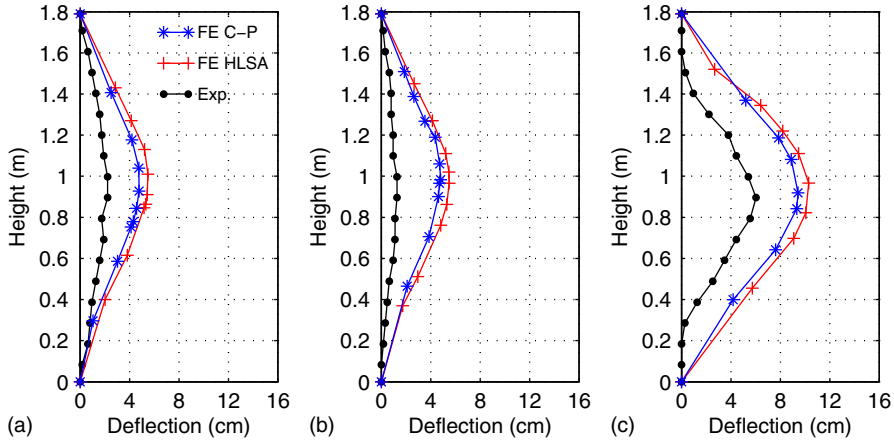

Fig. 14. Comparison of experimental results and FE simulation from Test 3 for Specimen 1L: (a) left flange deflection; (b) right flange deflection; (c) flange spread

at 6 and 30 m/s. The 6 m/s response has been included to illustrate the loss of web material. Table 2 presents a comparison of the dimensions of the rupture obtained from experimental testing and FE simulation using both the HLSA 350 data and the C-P model. In general, the results of the FE simulation agree reasonably well with the experimental results, with relative error for the height of the hole ranging from 11–13% (FE overestimating) and relative error for the width of the hole at approximately 31% (FE underestimating) by comparison to the experimental results.

A comparison of the global residual deformation of the W14 × 53 column obtained from the FE simulation and those measured following Test 1 are presented in Fig. 10. Figs. 10(a and b) present residual deflection data (cm) up the height of the column (m) measured from a reference plumb line to the front faces of the left and right flanges, respectively. The results plotted in Figs. 10(a and b) show that the HLSA 350 and C-P models produced similar results in terms of residual shape and magnitude, although both underestimated the experimental residual displacement. The relative error for the C-P model ranged from 33 to 39% for the peak flange out-of-plane residual displacement. Relative error for the HLSA 350 results ranged from 47 to 50% compared to the experimental data. A comparison of the face-to-face residual flange spread from FE simulation and tests is presented in Fig 10(c). The results plotted in Fig. 10(c) reinforce that the FE simulation with the HLSA 350 and C-P models produced similar results, although, again, both underestimated the experimentally observed residual displacements, with relative error for the peak values at approximately 16% for both HLSA 350 and C-P models.

Test 2: Specimen 2L

The partial rupture in the web of Specimen 2L was observed in the FE simulation and is shown in the FE rendering of the column in Fig. 11(b), taken at 12 m/s in the response. Rupture was also observed from the simulation using the HLSA 350 model, although it is not readily apparent from the rendering shown in Fig. 11(a). For comparison, a photograph of the partial rupture of the web on Specimen 2L is shown in Fig. 11(c).

A comparison of the residual deformation results obtained from the FE simulation with those obtained following Test 2 on Specimen 2L are plotted in Fig. 12. Residual deformation for the left flange, right flange, and centerline of web are presented in Figs. 12 (a, b, and c), respectively. For Test 2, the residual deformation results from the FE simulation using the C-P and HLSA 350 material models were similar in terms of trend and magnitude. However, the results of the FE simulations overestimated, to varying degrees, the experimentally observed values, with relative errors for peak left flange, right flange, and web deformations of approximately 280, 266, and 27%, respectively.

Test 3: Specimen 1L

Following Test 3, no material loss or rupture of the 1L specimen was observed. The results of the FE simulation also showed no material loss or rupture in the specimen. Renderings of the FE model presented in Fig. 13 show a similar deformation pattern to the observed bulge that was centered in the web at approximately midheight, as shown in the photograph in Fig. 13(c).

Fig. 14 presents a graphical comparison of the residual deformations results for Specimen 1L obtained from the FE simulation with the experimental results for Test 3. As with the previous comparison, the FE results overestimated the peak residual deformation in the left flange [Fig. 14(a)], right flange [Fig. 14(b)], and centerline of the web [Fig. 14(c)], with relative errors of 270, 116, and 57%, respectively.

Summary of Comparisons

The qualitative comparison of results presented in Figs. 9, 11, and 13 demonstrate that the FE modeling methodology qualitatively replicates the experimental results in terms of general deformation shape, magnitude of deformation, and observed damage. The quantitative comparison of results presented in Figs. 10, 12, and 14 suggests that FE simulation better replicates the local deformation and damage than the peak residual global deformation. For example, for Specimen 2R (Test 1), the FE simulations replicated the presence and size of the rupture hole (Table 2) and flange spread [Fig. 10(c)] with reasonable accuracy (i.e., <30% relative error), whereas the relative error for the peak residual deformation of the flanges (a measure of global deformation) ranged from 47 to 50% [Figs. 10(a and b)]. The same trend was observed for Tests 2 and 3, in which the relative error in the peak residual deformations of the flanges was much larger than for the webs.

Summary and Conclusions

Blast testing of three W14 × 53 propped cantilever columns was conducted to observe the deformation and failure modes for near

field high explosive detonations loading the column perpendicular to the weak axis of bending, and to collect residual deformation data. Data on global deformation were obtained by measuring residual out-of-plane (parallel to the strong axis of bending) deformations of the column flanges, whereas local deformation data were obtained by measuring residual centerline web deformations and face-to-flange spread.

FE simulation of the three tests was performed by using *LS-DYNA version 971*, considering two different material models: a data set from Yan and Urban (2003) for HLSA 350 and a semiempirical C-P model, both of which attempt to account for the strain rate effects on the steel material. Furthermore, the air surrounding the test specimens (fluid) was modeled by using an ambient area layer located near the section to reduce computational resources and time by not modeling the entire volume of air surrounding the charge, and importantly, between the charge and the specimen; however, attempts were made to capture fluid–structure interaction in the flange void. The CONWEP module was used to apply time and spatially varying pressures to the ambient air layer that were scaled to agree with pressures obtained from *BEL version 1.1.0.3*, which is able to account for cylindrically shaped charges like those used in the experimental testing portion of the study.

Based on the results of this study, the conclusions described in the following are offered.

- A high intensity, near field detonation producing large overpressures on the web of a wide flange column can result in highly localized web deformations, fractures along the web-to-flange joint, and/or create a hole in the column web (depending on the proximity of the charge); this indicates that loading perpendicular to the weak axis of bending is a critical scenario to be considered for the blast resistant design of wide flange columns.
- The FE modeling approach used in this study with *LS-DYNA version 971* was reasonably able to replicate the extent of breaching and lateral flange spread, i.e., deformation parallel to the weak axis of bending, for each test. However, the FE simulation was less successful in predicting global flange flexural deformations about the weak axis of bending with significant relative errors, particularly for Tests 2 and 3, in which the web remained partially or fully intact, i.e., relative error $>100\%$.
- Although there are insufficient data to draw a definitive conclusion regarding the large differences in global bending, a possible significant source for this discrepancy is the representation of the cylindrical shaped charge using a spherical air burst in CONWEP. It is also possible that some flexibility developed at the base of the test columns, especially given that localized crushing of concrete was observed at the base of the column following the tests. Refinements in modeling were not pursued, because simulation of local distortions was judged to be of more importance.
- FE simulation using *LS-DYNA version 971* was able to replicate the localized distortion and rupturing of the web of the wide flange section with reasonable accuracy using either the C-P material model or HLSA data from Yan and Urban (2003), suggesting that the modeling approach used in this study can provide an effective means of assessing the vulnerability of existing columns and of determining an appropriate section size for mitigating localized damage such as web rupture for exposed wide flange columns.

FE models, once calibrated, can be used to investigate how column global flexural stiffness interacts with local response and web breaching, which was beyond the scope of the current study.

Acknowledgments

This work was supported in part by the Earthquake Engineering Research Centers Program of the National Science Foundation under Award Number ECC-9701471 to the Multidisciplinary Center for Earthquake Engineering Research. However, any opinions, findings, conclusions, and recommendations presented in this paper are those of the authors and do not necessarily reflect the views of the sponsors. Special thanks are given to James C. Ray at the Eng. Research Dev. Center of the USACE for his help and assistance in the logistics of the experiments.

References

ASCE. (1997). "Design of blast resistant buildings in petrochemical facilities." Task Committee on Blast-Resistant Design, New York.

ASTM. (2011). "Standard specification for structural steel shapes." *A992*, West Conshohocken, PA.

Bridge Explosive Loading (BEL) version 1.1.0.3 [Computer software]. U.S. Army Corps of Engineers, Vicksburg, MI.

Dusenberry, D. (2010). *Handbook for blast resistant design of buildings*, Wiley, Hoboken, NJ.

Karagozian and Case. (2005). *Experimental results of the AISC full-scale column blast test*, AISC, Chicago.

LS-DYNA version 971 [Computer software]. Livermore Software Technology Corporation (LSTC), Livermore, CA.

Luecke, W. E., et al. (2005). "Federal building and fire safety investigation of the World Trade Center disaster: Mechanical properties of structural steels." *NIST NCSTAR 1-3D*, NIST, Gaithersburg, MD.

Pushkaraj, S., Whittaker, A. S., and Aref, A. J. (2010). "Modeling the effects of detonations of high explosives to inform blast-resistant design." *Technical rep. no. MCEER-10-0009*, Multidisciplinary Center for Earthquake Engineering Research, Buffalo, NY.

United States Department of Defense (DoD). (2008). "Design of structures to resist the effects of accidental explosions." *Rep. No. UFC-3-340-02*, Washington, DC.

Warn, G. P., and Bruneau, M. (2009). "Blast resistance of steel plate shear walls designed for seismic loading." *J. Struct. Eng.*, 10.1061/(ASCE)ST.1943-541X.0000055, 1222–1230.

Williamson, E. B., and Winget, D. G. (2005). "Risk management and design of critical bridges for terrorist attacks." *J. Bridge Eng.*, 10.1061/(ASCE)1084-0702(2005)10:1(96), 96–106.

Yan, B., and Urban, D. (2003). "Characterization of fatigue and crash performance of new generation high strength steels for automotive applications." *Final Rep.*, American Iron and Steel Institute, East Chicago, IL.